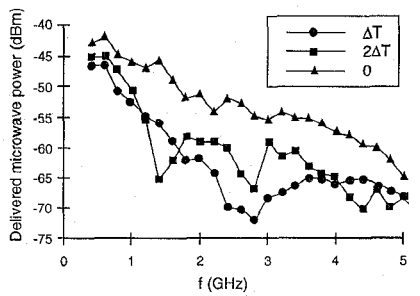

CThM1 Fig. 2. Variations in the delivered microwave power with the modulation frequency for the three configurations: no grating (ΔT), sum of optical and electrical delays ($2\Delta T$), and cancellation of the delays (0), i.e., synchronism of the photogenerated microwave signal with the optically carried microwave signal. Average incident optical power $P_{opt} = 0.1$ mW.

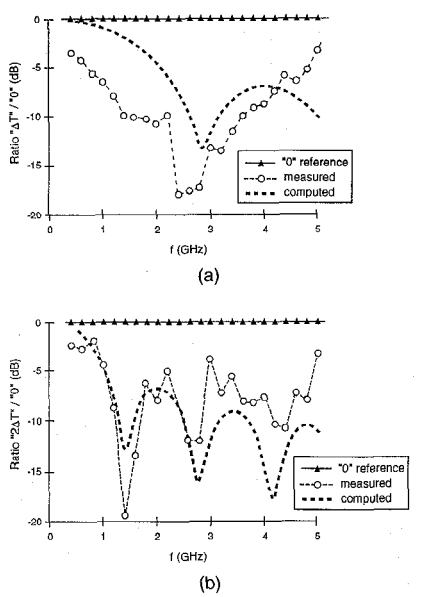

CThM1 Fig. 3. Measured and computed ratio of the microwave powers delivered in the three configurations of Fig. 2. The «0» configuration is considered as a reference. (a) Ratio of the microwave powers delivered in the «ΔT» and «0» configurations. (b) Ratio of the microwave powers delivered in the «$2\Delta T$» and «0» configurations.

affect the photodetection efficiency showing minimas at 1.4, 2.8, and 4.2 GHz. This preliminary experiment appears to be in good agreement with the numerical simulation, which is also discussed, in addition to further optimizations of the device.

**Present address: Thomson-CSF AIRSYS, Limours, France*

1. K.S. Giboney, M.J.W. Rodwell, J.E. Bowers, IEEE Photonics Technol. Lett. **4,** 1363 (1992).
2. L.Y. Lin, M.C. Wu, T. Itoh, T.A. Vang, R.E. Muller, D.L. Sivco, A.Y. Cho, IEEE Photonics Technol. Lett. **8,** 1376 (1996).
3. D.P. Prakash, D.S. Scott, H.R. Fetterman, M. Matloubian, Q. Du, W. Wang, IEEE Photonics Technol. Lett. **9,** 800 (1997).
4. H. Jiang, J.T. Zhu, A.L. Kellner, P.K.L. Yu, Proc. SPIE, **2844,** 120 (1996).
5. S. Jasmin, N. Vodjdani, J.-C. Renaud, A. Enard, IEEE Trans. Microwave Theory Tech. **45,** 1337 (1997).

CThM2 10:45 am

Saturation characteristics of fast photodetectors

Pao-Lo Liu, Michael Y. Frankel, Keith J. Williams, Ronald D. Esman, *Code 5672 Naval Research Laboratory, 4555 Overlook Avenue, SW, Washington, D.C. 20375*

Photodetector saturation can limit the performance of high-power, high-frequency analog systems. Photodetectors saturate primarily because of space charge, which redistributes the electric field within the intrinsic region, resulting in reduced output and a sharp increase in harmonic distortion.[1]

Photodetector saturation has been measured in the frequency domain using the heterodyne technique, where, for 18-GHz bandwidth devices, the saturation current at 10 GHz is typically 2–15 mA[2]. Alternatively, short laser pulses can be used to characterize the peak saturation current of photodetectors in the time domain. A peak saturation current of 56 mA has been reported for a velocity-matched distributed photodetector.[3] The issue has been in reconciling time-domain measurements with those of frequency domain, with the former typically producing significantly higher saturation currents. Here, we report measurements of photodetector saturation current in both the time and frequency domains.

In time-domain measurements [Fig. 1(a)], a 1560-nm mode-locked fiber laser generates 3-ps pulses at a 40-MHz repetition rate. Single-mode fiber segments are used to disperse the pulse to 33, 75, and 220 ps, respectively. The pulse passes through an in-line attenuator and a 10–90 power splitter for monitoring and power control, respectively, before impinging on a pigtailed photodetector connected to a 50-GHz sampling oscilloscope. Two p-i-n

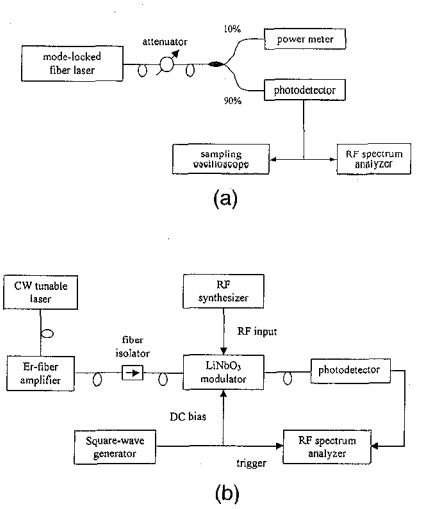

CThM2 Fig. 1. Schematic diagram of time-domain (a) and frequency-domain (b) measurement configurations.

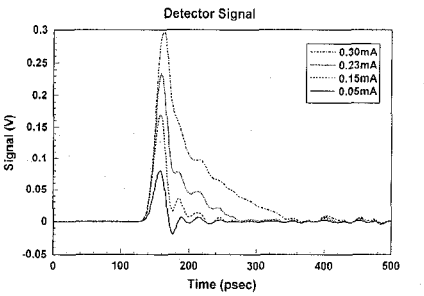

CThM2 Fig. 2. Picometrix p-i-n photodetector output at four different power levels. As the average current increases from 0.05 to 0.30 mA, the peak of the signal becomes saturated while an extended tail appears. Between the detector and the sampling oscilloscope, there is a 26-dB attenuator.

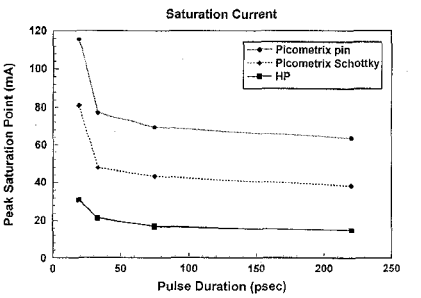

CThM2 Fig. 3. The peak saturation current as a function of pulse duration for three fast photodetectors. A higher saturation current is observed for short pulses.

photodetectors from Picometrix and Hewlett-Packard with an FWHM impulse response of 19 and 23 ps, respectively, and a Schottky photodetector from Picometrix with a response of 22 ps have been measured. A typical response (Fig. 2) shows that an extended tail appears as the photodetector saturates. For pulsed measurements, the 1-dB compression current is defined as the peak current at which the response deviates by 1 dB from the expected linear response. After compensating for the response of the sampling system, the measured 1-dB compression current (Fig. 3) is seen to be a function of pulse duration. For very short pulses, the space charge takes time to evolve and has less effect on the peak of the pulse, therefore recording a higher saturation current. Preliminary simulations of the nonlinear transport equations indicate space-charge field buildup of 6–9 ps.

In frequency-domain measurements [Fig. 1(b)], a 200-mW fiber-amplified 1550-nm cw diode laser is small-signal rf modulated by a Mach–Zehnder modulator (MZM). The MZM dc bias port is used to switch between the minimum transmission and the quadrature points. The photodetector is connected to an rf-spectrum analyzer. The 1-dB compression current is defined as the dc photocurrent at which the rf power is compressed by 1 dB. For the Hewlett–Packard p-i-n device at 10.2 GHz, the 1-dB compression point occurs at 5 mA, in contrast to as much as 30 mA of peak saturation photocurrent under pulse conditions. Frequency-domain measurements con-

sistently produce lower compression currents than time-domain measurements for all tested photodetectors. The difference can be explained by the delayed evolution of the space-charge field and by the fact that saturation is frequency dependent. High-frequency signals become saturated at much lower levels than low-frequency signals. Frequency-domain measurements are usually performed at high frequencies, whereas time-domain measurements represent the average saturation level over a broad frequency range. We report details of measurements, including the bias dependence, simulation results, buildup time of the space-charge field, and comparison between the time- and frequency-domain measurements.

1. K.J. Williams, R.D. Esman, M. Dagenais, J. Lightwave Technol. **14,** 84 (1996).
2. K.J. Williams, R.D. Esman, S. Williamson, J. Valdmanis, K. Al-Hemyari, J.V. Rudd, IEEE Photonics Technol. Lett. **9,** 812 (1997).
3. L.Y. Lin, M.C. Wu, T. Itoh, T.A. Vang, R.G. Muller, D.L. Silva, A.Y. Cho, IEEE Photonics Technol. Lett. **8,** 1376 (1996).

CThM3 **11:00 am**

Long-wavelength velocity-matched distributed photodetectors

T. Chau, L. Fan, D.T.K. Tong, S. Mathai, M.C. Wu, D.L. Sivco,* A.Y. Cho,* *UCLA, Electrical Engineering Department, 66-147D Engineering IV, Box 951594, Los Angeles, California 90095-1594; E-mail: wu@ee.ucla.edu*

High-power, high-speed photodetectors are a key component in microwave fiber-optic links, optoelectronic generation of microwaves, and millimeter waves.[1] Previously, we have reported a GaAs/AlGaAs velocity-matched distributed photodetector (VMDP) that operates at 860 nm and demonstrated its potential for high-saturation photocurrents.[2] For applications in rf photonic systems, however, InP-based long-wavelength photodetectors operating at 1.3 or 1.55 μm are required. In this paper, we report on the experimental results of InGaAs/InAlGaAs/InP VMDP.

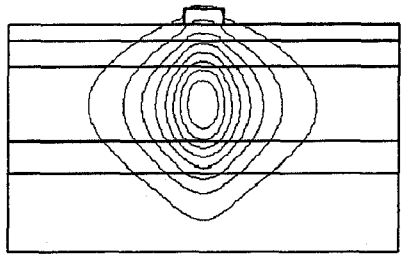

CThM3 Fig. 2. Contour plot of the fundamental mode field amplitude in the passive optical waveguide using BPM simulation. See Fig. 1 for layer structure.

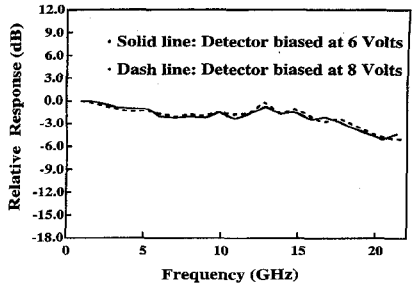

CThM3 Fig. 3. Measured frequency response of long-wavelength VMDP (12 photodiodes, 1.2 mm long).

The schematic structure of the VMDP is illustrated in Fig. 1. Active metal-semiconductor-metal (MSM) photodiodes are periodically distributed on top of a passive optical waveguide. Optical signal is evanescently coupled from the passive waveguide to the active MSM photodiodes. Photocurrents generated from each MSM photodiode are added in phase through a 50-Ω coplanar strip (CPS) microwave transmission line that is velocity matched to the optical waveguide. The MSM photodiodes serve two functions here: they generate photocurrents and provide the periodic capacitance loading needed for velocity matching. The VMDP design allows the passive waveguide, the active photodiodes, and the microwave coplanar strips to be independently optimized. In Fig. 1, the active MSM photodiode consists of an InGaAs absorption layer, an InGaAs/InAlAs graded superlattice layers, and an InAlAs Schottky-barrier enhancement layer. At 10-V bias, a dark current of 190 pA is measured for an 11 × 48-μm^2 MSM photodiode. For a 1.2-mm-long VMDP with 12 11 × 48-μm^2 MSM photodiodes, a dark current of 25 nA is measured at 10-V bias.

Figure 2 shows the contour plot of the fundamental mode field amplitude in the passive waveguide using beam propagation method (BPM) simulation. The VMDP is designed so that only the fundamental mode exists in the optical waveguide and the active photodiode regions. Simulation results with the BPM method indicate a 4% scattering loss and 7% absorption loss per photodiode. Scattering loss can be reduced to 1% per diode by optimizing the geometric structure of the active photodiode. The device under test is 1.2 mm long and consists of 12 MSM photodiodes. In this experiment, optical lithography is employed to pattern the MSM photodiodes. Both the fingers and the spacing are 1 μm wide. After antireflection (AR) coating, a quantum efficiency of 34% was measured (this includes the coupling loss from optical fiber). High-saturation current measurement with a high-power erbium-doped fiber amplifier is in progress.

The frequency response of the VMDP is characterized by the optical heterodyne method.[4,5] The system consists of two external cavity tunable lasers at 1.55 μm; the frequency of each laser can be tuned in 1-GHz steps. The optical signals are combined by a 3-dB coupler and coupled to the VMDP through a fiber pickup head. The microwave signal generated by optical mixing in the VMDP is collected at the output end of the CPS by a 50-GHz picoprobe (GGB Industries), which is connected to an rf-power sensor and monitored by an rf-power meter. The calibrated frequency response of long-wavelength VMDP is shown in Fig. 3. A 3-dB bandwidth frequency of 18 GHz is measured. By scaling down the MSM to 0.1 μm scale, a frequency response >100 GHz is expected.

In summary, we have experimentally demonstrated a high-speed, high-power long-wavelength VMDP using optical lithography. A 3-dB bandwidth of 18-GHz and an overall quantum efficiency of 34% have been achieved.

This project is supported by TRW, ONR MURI on RF Photonics, ARO, JSEP, and UC MICRO.

Lucent Technologies, Bell Laboratories, Murray Hill, New Jersey 07974

1. C.H. Cox III, IEEE Proc. J. **139,** 238–242 (1992).
2. L.Y. Lin, M.C. Wu, T. Itoh, T.A. Vang, R.E. Muller, D.L. Sivco, A.Y. Cho, IEEE Trans. Microwave Theory Tech. **45,** 1320–1331 (1997).
3. H. Kogelnik, "Theory of optical waveguides," in *Guided-Wave Opto-Electronics,* T. Tamir, ed. (Springer-Verlag, Berlin, 1988).
4. T. Hawkins II, M.D. Jones, S.H. Pepper, J.H. Goll, J. Lightwave Technol. **9,** 1289–1294 (1991).
5. P.D. Hale, D.A. Humphreys, A.D. Gifford, SPIE **2149,** 345–356, 1994.

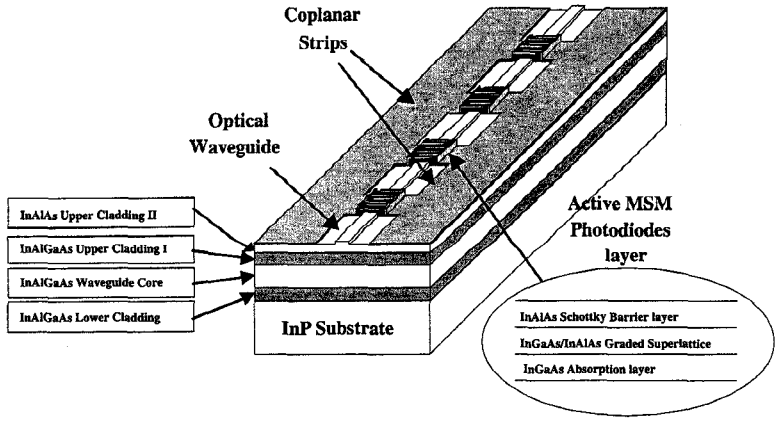

CThM3 Fig. 1. Schematic structure of long-wavelength velocity-matched distributed photodetector (VMDP).